Aust. J. Phys., 1985, **38**, 633–46

Self-draining Manifolds for Solar Collectors

R. C. McPhedran, I. C. Onley, D. R. McKenzie and R. E. Collins

Solar Energy Group, School of Physics,
University of Sydney, Sydney, N.S.W. 2006.

Abstract

We consider manifolds for solar collectors capable of self-draining action as a means of freeze protection. We study a number of single- and double-header designs, both in the context of domestic and industrial installations. We present both simple theoretical models and experimental results for various promising manifold designs, indicating optimal choices for key design parameters.

1. Introduction

Solar collectors are now used in a wide variety of climatic zones varying from tropical to near-arctic regions. It is neither practical nor economical to design a single collector system suitable for such a wide range of conditions, so that the collector design will depend on the operational environment. One important problem in cold climates is that of protecting the collector from damage due to the freezing of its heat extraction fluid. This can be done by adding a suitable anti-freeze chemical to the fluid. Another method of freeze protection is the complete removal ('drain-down') of the fluid from the collector manifold whenever its temperature rise on passing through the collector is less than a pre-determined value.

One disadvantage of using anti-freeze in solar collectors heating domestic water is the increased system complexity required to guarantee purity of potable water. Also, the exposure of the collector fluid to low ambient temperatures during extended periods causes substantial heat loss and reduces system efficiency. On the other hand, the drain-down method must be completely reliable if the system lifetime is not to be curtailed. Hence, it is desirable to achieve drain-down by passive rather than active means. Manifolds which achieve this are termed self-draining; they do not require a heat exchanger and can be significantly more efficient than systems employing anti-freeze liquid (Dubin and Bloome 1981).

There are numerous ways of designing self-draining manifolds for solar collectors, but a convenient way of classifying them is into single- and double-header types. In the former, liquid flows into riser pipes from a header pipe, absorbs thermal energy and is returned to the same header pipe. In the latter, the heated liquid is collected by a second header pipe. Here, we discuss designs of both types, concentrating on

0004-9506/85/040633$02.00

manifolds for evacuated tubular collectors (Kreith and Kreider 1981). However, our results also have relevance to the design of manifolds for flat-plate collectors.

Important design characteristics which we consider are the distribution and stability of flow among the various risers of the manifold, head loss around the manifold, and the efficiency of the self-draining action. We discuss the single- and double-header manifolds both in the context of a small domestic installation and a medium-scale industrial system. We present both theoretical models and experimental results for a number of promising manifold designs.

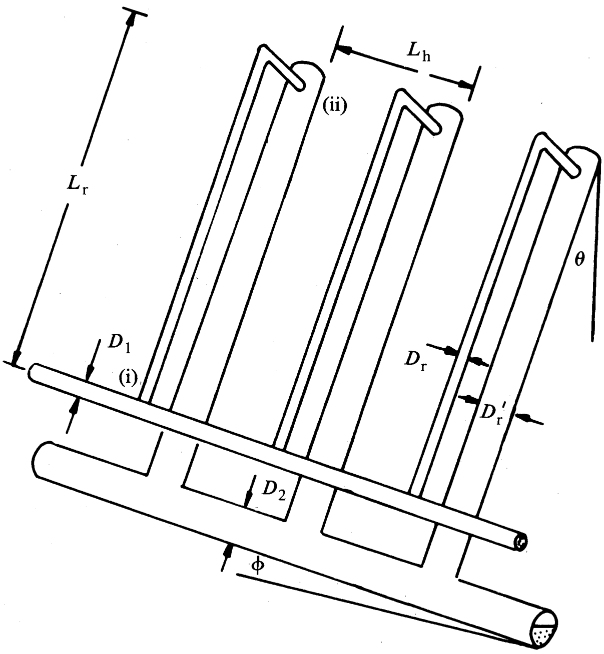

Fig. 1. Self-draining double-header manifold, showing the characteristic diameters D_1, D_2, D_r and D_r', the lengths L_h and L_r and the inclination angles θ and ϕ.

2. A Double-header Manifold

We consider the self-draining manifold shown schematically in Fig. 1. Water enters the manifold through an inlet header of internal diameter D_1, along which risers are connected in parallel separated by an interval L_h. Water coming from the inlet header first ascends a pipe of small diameter D_r, inclined at an angle θ to the vertical, before falling under gravity through a pipe of larger diameter D_r' into the outlet header. This outlet header has an internal diameter D_2 and is inclined at an angle ϕ to the horizontal.

During normal or pumped operation of this manifold, the inlet header and inlet side of the riser pipes have closed-channel flow, while the outlet portion of each riser and the outlet header have open-channel flow. When pumping stops, back flow of air through the outlet header and riser sections enables complete draining under gravity of the inlet riser sections and the inlet header.

This design is based on commercially developed manifolds for tubular solar collectors. However, it is commercial practice to use the inner glass walls of the evacuated tubes as part of the water containment circuit, while in the manifold of Fig. 1 water is entirely contained in metal pipes, with a heat transfer fin providing thermal contact between the collector tubes and the risers.

In previous work (McPhedran *et al.* 1983) we studied the forced isothermal flow of water through a parallel connected manifold of the non-self-draining type. We have adapted the previous formulation to study the isothermal flow through the manifold of Fig. 1, with the aim of optimizing the various critical design parameters. We will not discuss the new formulation in detail here, but give the key equations in Appendix 1. The interested reader will find fuller details in McPhedran (1983).

Numerical studies have been made to determine the appropriate values for key manifold parameters (D_r, D_r', D_1, D_2 and ϕ), both for a small domestic installation and for an industrial system. The other manifold parameters (L_r, L_h and θ) are fixed by the size of the evacuated tubes, the optical design of the solar panel and the latitude of the installation.

The choice of manifold parameters for the system of Fig. 1 breaks up into three separate problems. In the first, D_1 and D_r are chosen so that flow in the inlet risers is sufficiently uniform (i.e. so that the ratio of maximum to minimum riser volume flow rates is smaller than 2). Also, adequate flow rates must be maintained in each riser (with the temperature increase in the riser ΔT_r always being smaller than 5 K). In the second problem, the diameter D_r' is chosen to ensure open-channel flow in each outlet riser. Thirdly, the diameter D_2 and the inclination angle ϕ are chosen to ensure open-channel flow in the outlet header.

Flow in the Inlet Section of Risers

Flow characteristics were calculated for a domestic system having 32 risers, operated at 60°C and with a volume flow rate Q_h^1 at the entrance to the manifold of 10^{-4} $m^3 s^{-1}$. Five values were chosen for the internal diameter of the inlet header D_r (stepping from 1 to 5 mm) and D_1 was varied between 10·9 and 48·4 mm.

For D_r equal to 1 or 2 mm, all header diameters considered gave acceptable flow ratios. For D_r equal to 3, 4 and 5 mm the smallest acceptable values of D_1 are respectively 17, 23 and 29 mm.

For a fixed value of D_1, decreasing the value of D_r results in a more uniform distribution of riser flow. However, if we decrease D_r too far then the pump power required to force water through the risers becomes unacceptably large. Also, with small values of D_r there is an increased risk of riser blockage due to trapped sediment in the circulating water. For these reasons, we select 3 mm as a reasonable minimum value for the internal diameter of the inlet riser.

Flow characteristics were also calculated for an industrial system having 160 risers, operated at 60°C and with Q_h^1 equal to 5×10^{-4} $m^3 s^{-1}$. For D_r equal to 3, 4 and 5 mm the smallest acceptable values of D_1 are respectively 29, 29 and 42 mm.

Flow in the Outlet Section of Risers

Having obtained appropriate values for the diameters D_1 and D_r, we consider the problem of choosing the diameter D_r' of the outlet section of the risers. The diameter is required to be large enough so that water entering the outlet section will be carried away sufficiently quickly by gravity to ensure open-channel flow. A simple argument suffices for a minimum value of D_r', provided that surface tension effects are negligible.

Let us calculate the distance s water would have to fall from rest in a pipe of diameter D_r' before the fluid flow rate reached a value Q_r (assuming the pipe to be completely filled by falling water). At greater distances down the pipe, it would only be partially filled by the falling water. From elementary dynamics we have

$$v_r'^2 = (4Q_r/\pi D_r'^2)^2 = 2gs\,, \tag{1}$$

where g is the acceleration due to gravity. We ensure open-channel flow by requiring s to be only a small fraction of the diameter D_r' (i.e. $s = D_r'/F$). Then from (1) we get

$$D_r' = \left(\frac{4Q_r}{\pi(2g)^{\frac{1}{2}}}\right)^{\frac{2}{5}} F^{\frac{1}{5}}\,. \tag{2}$$

Experiments have been performed to determine suitable values for the factor F. This increases with decreasing pipe diameter (as surface tension effects increase the tendency to closed-channel flow). For pipes of internal diameter 11 mm, F is around 5, while for D_r' equal to 7 mm, F is around 8.

Flow in the Outlet Header

Finally, we consider the choice of the internal diameter D_2 and pitch angle ϕ of the outlet header. Let A denote the flow area, which is a function of the distance l down the outlet header. The flow starts at $l = 0$ and when l reaches the total header length l_h it has attained the volume flow rate Q_h. An adequate diameter D_2 will be such that for all points in the outlet header

$$A \leqslant \tfrac{1}{4}\pi D_2^2\, S_F\,. \tag{3}$$

Here S_F is the safety factor, for which we will adopt the value 0·75. At least 25% of the outlet header area is then available for air flow to or from the risers.

We have used a continuous model for flow in the outlet header, based on conservation of momentum rather than mechanical energy at riser/header junctions. The analysis given in McPhedran (1983) leads to the result

$$D_2 \geqslant \left(\frac{4Q_h}{\pi S_F}\right)^{\frac{1}{2}} \left\{\left(3 + \frac{16\pi\mu\, l_h}{\rho Q_h}\right)\Big/ 2g l_h \sin\phi\right\}^{\frac{1}{4}}. \tag{4}$$

Here μ and ρ denote respectively the viscosity and density of water.

As a sample of the use of (4), for a domestic manifold with 32 risers operated at 60°C with $Q_h = 7\times10^{-5}\ \mathrm{m^3\,s^{-1}}$ and $\phi = 3{\cdot}3°$, we find that D_2 must not be smaller than $1{\cdot}69\times10^{-2}$ m. For an industrial manifold with 160 risers and $Q_h = 3{\cdot}5\times10^{-4}\ \mathrm{m^3\,s^{-1}}$ we find from (4) a lower bound on D_2 of $2{\cdot}63\times10^{-2}$ m. These diameters agree well with those obtained as a result of field tests on similar manifolds (M. Platt, personal communication 1983).

Practical Operation of the Manifold

In order to test flow balancing and drain-back characteristics of the manifold of Fig. 1, a set of risers was constructed in clear plastic tubing, the risers being linked by copper header pipes. At low flow rates this manifold operated in a satisfactory fashion, with equal flow in all risers and open-channel flow in the outlet section of each. However, once a riser flow rate exceeded the value Q_r obtained from (2), then all air was excluded from that riser, reducing head loss in it and further increasing Q_r. This process continued until one riser operated with closed-channel flow, and neighbouring risers were completely starved of flow. Once the manifold was in this undesirable condition, it was only possible to restore flow balance by either draining it completely, or by increasing the flow rate to unacceptably high values.

This potential instability of the manifold places tight tolerances on the uniformity of its construction, and on the total flow rate Q_h^1, if it is used close to its design limits. Careful design of the recirculating system is then necessary to avoid transient effects on re-filling of the manifold, which may force it into the closed-channel flow-starved configuration described above.

When closed-channel flow occurs in a riser, the pressure at the junction point between the inlet and outlet sections falls below the atmospheric value. Hence, it is possible to prevent the occurrence of this condition by making a small hole at the top of the outlet section of the riser. We have verified experimentally that such holes prevent the onset of closed-channel flow, irrespective of the riser flow rate.

The drain-back characteristics of the manifold of Fig. 1 were seen experimentally to be entirely adequate. The speed of drain-back was improved by the insertion of a hole in each outlet riser.

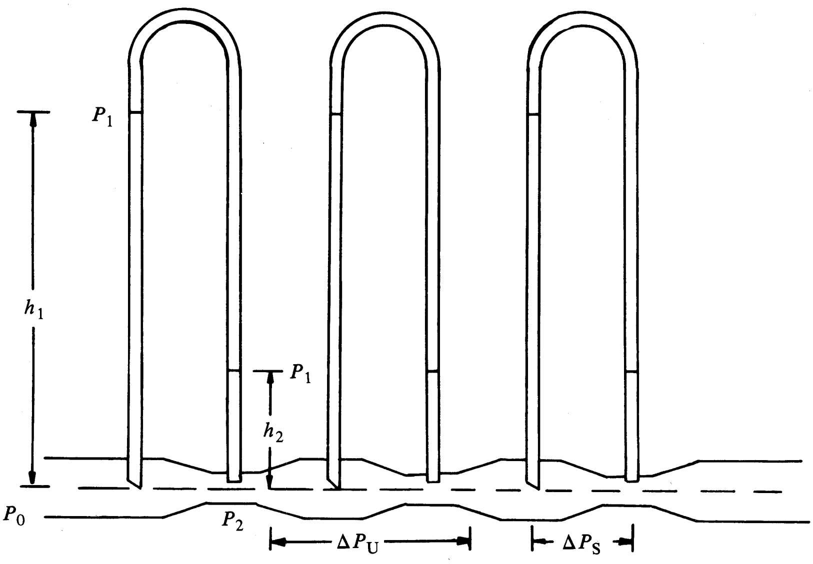

Fig. 2. Self-draining single-header manifold, where the section shown has its risers tilted along their length at an angle θ to the vertical. Flow in the header is from left to right. Shown are the heads h_1 and h_2, the pressures P_0, P_1 and P_2 and the pressure differences ΔP_U and ΔP_S.

3. Single-header Manifolds

Here we consider manifolds in which all risers take fluid from and return fluid to a single-header pipe. In this configuration, identical risers have identical flow rates, irrespective of their location along the header pipe. A balanced, stable flow pattern is thus a consequence of this design. Also, if the risers are placed above a slightly inclined header pipe, drain-back will occur.

We consider the manifold of Fig. 2, which is being refilled after drain-back. Flow will only start in a riser when the liquid in its inlet arm has reached the top of the riser, a height $L_r \cos\theta$ above the header. Once this level has been achieved, closed-channel flow will be initiated in the riser. From Fig. 2, we see that if the pressure difference ΔP_S between the ends of the riser exceeds $\rho g L_r \cos\theta$ then flow will occur in that riser.

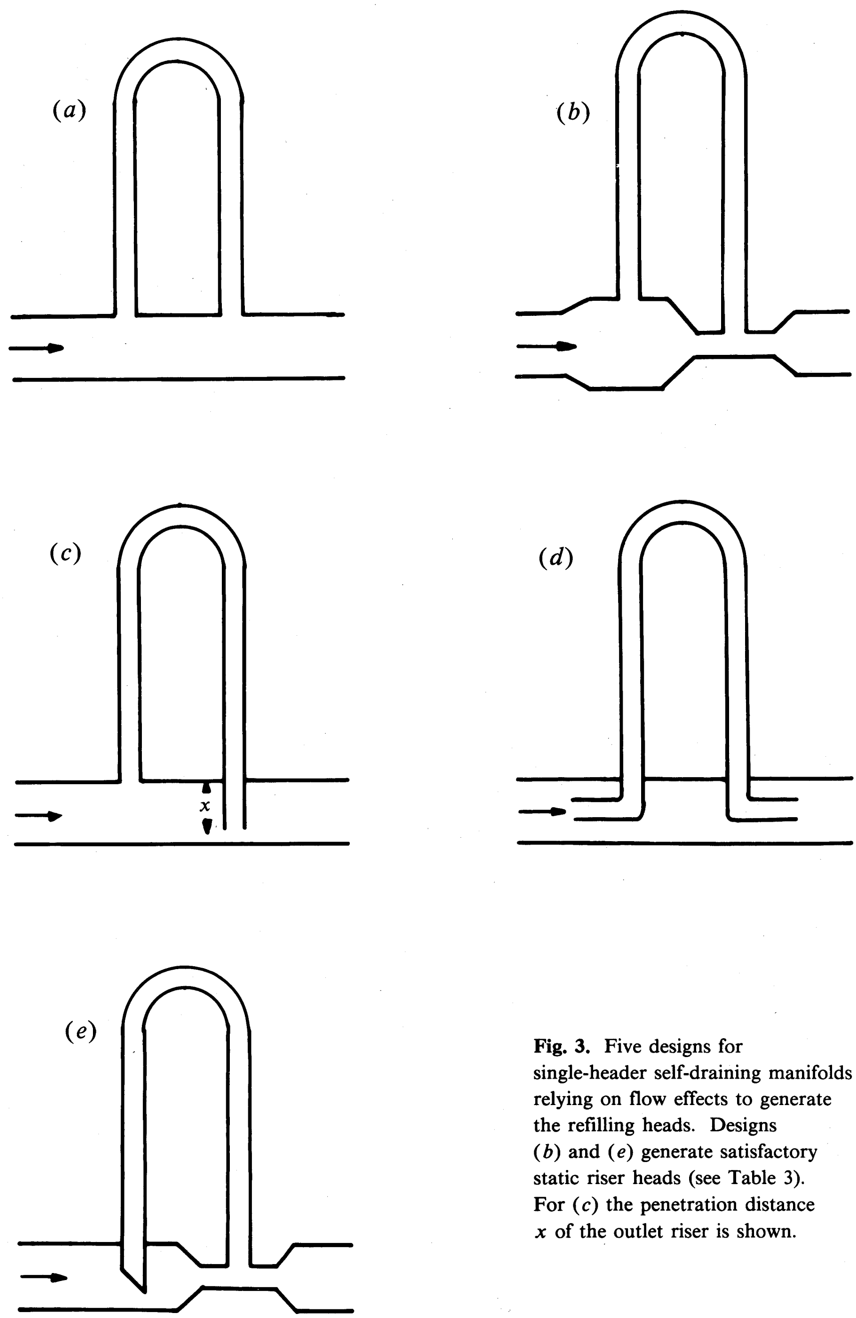

Fig. 3. Five designs for single-header self-draining manifolds relying on flow effects to generate the refilling heads. Designs (*b*) and (*e*) generate satisfactory static riser heads (see Table 3). For (*c*) the penetration distance *x* of the outlet riser is shown.

The pressure difference along the header pipe required to refill all N risers is $N\Delta P_U$. In order to minimize the size and power requirements on the recirculating pump, we must design our manifold in order to maximize its pressure-advantage ratio $\beta = \Delta P_S/\Delta P_U$.

We now consider a number of designs (Fig. 3) for single-header self-draining manifolds. These all use pressure differences associated with liquid flow in a changing geometry in order to stimulate flow in the risers. As we shall see, it is important to distinguish two types of pressure difference. The first we call reversible, which is associated with the conversion of kinetic energy into momentum flow, and vice versa. The second is irreversible, and is associated with the conversion of kinetic energy into heat. Good manifold designs attain substantial values of β by maximizing the reversible contribution to pressure differences.

We present a theoretical analysis of the flow properties of the designs in Figs 3*a* and 3*b*. The analysis is intended as a guideline to suitable choices of the manifold parameters, rather than constituting a rigorous formulation of the flow problem. We base the analysis on empirical data from the fluid engineering literature (Hansen 1967; Swanson 1970; Miller 1978; Ward-Smith 1980), rather than attempting exact calculations which would be mathematically abstruse and probably uninformative on the practical plane. Our formalism is sufficiently simple to be readily understood and, as we shall see, sufficiently realistic to be valuable in practical manifold design.

We give experimental results for all the designs shown in Fig. 3. While these designs do not exhaust all the possibilities for efficient single-header manifolds, they have all been chosen on the basis of ease of manufacture.

Theoretical Analysis of a Single-header Manifold

We consider then the manifold shown in Fig. 4 in which the flow speeds ($\overline{v}_1$ to $\overline{v}_5$ and $\overline{v}_r$), lengths (L_1 to L_9) and internal pipe areas (A_1 to A_3 and A_r) are introduced. The flow problem for this manifold may be reduced to one of determining $\overline{v}_3$ and $\overline{v}_r$, given $\overline{v}_2$. Key equations for the solution of this flow problem are presented in Appendix 2; here we only outline the theoretical method and its principal results.

The pressure difference $P_3 - P_6$ between $x = L_3$ and L_6 may be obtained in two ways. The first involves fluid passing through the riser, and gives $P_3 - P_6$ as a monotonically increasing function of $\overline{v}_r$. The second involves fluid passing through the header and gives $P_3 - P_6$ as a monotonically increasing function of $\overline{v}_3$. The equation for continuity of flow links $\overline{v}_3$ and $\overline{v}_r$ to $\overline{v}_2$. A bisection method may be used to find the value of $\overline{v}_3$ which makes the two expressions for $P_3 - P_6$ equal. Given $\overline{v}_3$, flow rates and pressure drops everywhere along the manifold can be readily calculated. The most important pressure drops are $\Delta P_t = P_9 - P_0$ and $\Delta P_r = P_6 - P_3$, which we will specify by giving the associated head losses h_t and h_r.

As well as calculating head differences with flow in the risers, it is important to calculate them when the manifold is being refilled, so that $\overline{v}_r$ is zero. We denote the head losses from $x = L_0$ to L_9, and from $x = L_3$ to L_6 in this situation by h_u and h_s respectively. Formulae for h_u and h_s have been given by McPhedran (1983).

Both ratios h_r/h_t and h_s/h_u could be adopted as figures of merit for manifold designs. However, our theoretical and experimental studies of the manifold of Fig. 4 have shown these two ratios to be approximately equal, so that they can be used interchangeably.

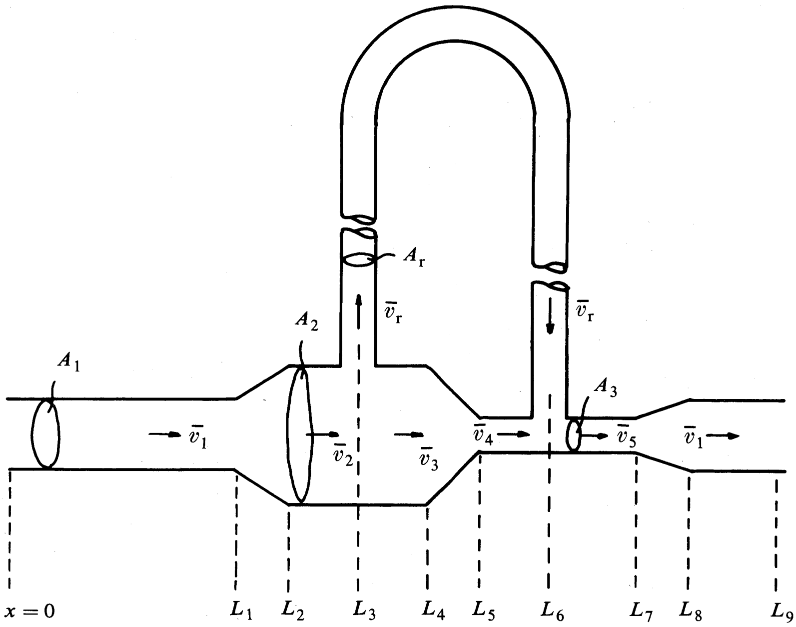

Fig. 4. A section of a single-header manifold showing the definition of the lengths L_1 to L_9, the internal cross-sectional areas A_1, A_2, A_3 and A_r, and the flow speeds $\bar{v}_1$ to $\bar{v}_5$ and $\bar{v}_r$.

We consider flow in a manifold having quite small changes in diameter, such as might be readily introduced by manufacturing errors. In Fig. 4, we take D_2/D_1 and D_3/D_1 to be respectively $1 \cdot 05$ and $0 \cdot 95$. At a suitable total flow rate for the domestic system ($Q_h^1 = 4$ L min^{-1}) the riser flow rate is too small (the temperature increase ΔT_r for 40 W thermal input into the circulating fluid per riser being 72°C). However, at a suitable total flow rate for the industrial system (20 L min^{-1}), the riser flow rate is sufficiently large (ΔT_r being 3°C). The corresponding value of h_s for the industrial system is only 5 cm, whereas a head of $1 \cdot 03$ m would be required to refill a riser $1 \cdot 45$ m long inclined at 45° to the vertical. This design illustrates that the achievement of static heads large enough to permit filling of the risers is a much more stringent requirement than obtaining adequate flow rates in the filled risers. It also enables us to rule out the design of Fig. 3*a* for a self-draining manifold.

For purposes of generality, we have included two diffusers (i.e. diameter increases) in the manifolds of Figs 3*b* and 4. However, the diffuser lying between $x = L_1$ and L_2 in Fig. 4 makes effectively no contribution to h_r, while it does increase h_t. Our numerical studies have shown that this diffuser only serves to worsen manifold performance.

Theory versus Experiment for a Single-header Manifold

In Fig. 5*a* we compare theoretical and experimental values of h_s and h_u, the manifold being that of Figs 3*b* and 4 and having $D_1 = D_2 = 1 \cdot 71$ cm and $D_3 = 0 \cdot 64$ cm. The calculated and measured values for h_s agree very well, but the theoretical estimates of h_u are significantly smaller when compared with experiment. This indicates that the friction factors f and geometrical loss factors K_C and K_D discussed in Appendix 2 are probably underestimates.

The system of Fig. 5*a* has an appropriate design for a domestic manifold. In order to generate the head of $1 \cdot 03$ m required to refill risers after drain-back the required total flow rate is 8 $\mathrm{L\,min^{-1}}$. Other performance details of this manifold are given in Table 1.

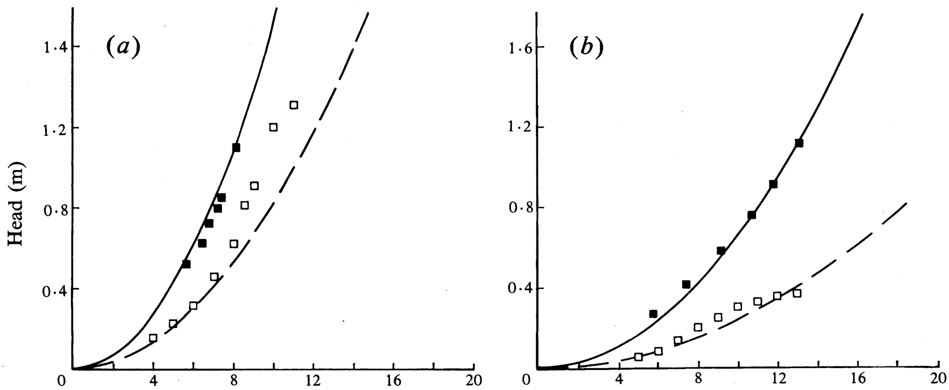

Fig. 5. Riser-static heads are shown as a function of volume flow rate for a single-header manifold with $D_1 = D_2 = 1 \cdot 71$ cm: (*a*) $D_3 = 0 \cdot 64$ cm and (*b*) $D_3 = 0 \cdot 80$ cm. The solid curves and filled squares show theoretical and measured values of the riser head h_s, while the dashed curves and unfilled squares show theoretical and measured values of total head loss h_u.

Table 1. Comparison of single- and double-header domestic and industrial systems

Here DDH denotes a domestic double-header manifold with $D_r = 3$ mm, $D'_r = 7$ mm, $D_1 = 1 \cdot 70$ cm and $D_2 = 1 \cdot 69$ cm. IDH denotes an industrial double-header manifold with $D_r = 3$ mm, $D'_r = 7$ mm, $D_1 = 2 \cdot 30$ cm and $D_2 = 2 \cdot 63$ cm. The domestic single-header manifold (DSH) has $D_1 = D_2 = 1 \cdot 71$ cm, $D_3 = 0 \cdot 635$ cm and $D_r = 4 \cdot 4$ mm. The industrial single-header (ISH) manifold has $D_1 = D_2 = 1 \cdot 71$ cm, $D_r = 4 \cdot 4$ mm and $D_3 \approx 1 \cdot 1$ cm

System	Flow rate ($\mathrm{L\,min^{-1}}$)	ΔT_m[D] (°C)	ΔT_r (°C)	Power delivered by pump (W)	Refilling head (m)
DDH	3·6	5·2	<5·5	0·65	1·10
DSH	4[B]	1·7	4·7	3·35	5·12
	8[C]			26·4	20·2
IDH	18	5·2	<6·6	3·41	1·16
ISH[A]	20	4·7	1·0	105	32·0
	28			227	49·6

[A] The industrial single-header values are experimental; the other values are calculated.
[B] Operation. [C] Refilling. [D] ΔT_m is the temperature rise across the manifold.

In Figs 5*b* and 6 we compare theoretical and experimental values of riser-static head for manifolds with D_3 equal to 8 and 10 mm respectively. In the former case, agreement between theory and experiment is good, both for h_s and h_u (with the theoretical value being slightly too low for the total head), while in the latter the theoretical curves for D_3 equal to $10 \cdot 3$ mm lie between the experimental head values for D_3 equal to 10 and 12 mm. These measurements demonstrate clearly the sensitivity of manifold pressure to small changes in D_3. We note also that the actual profile of the pipe construction varies between theory and experiment. The technique used to form the constriction was to crimp down the copper tubing around a steel rod, giving a pipe profile only approximately like the idealized form of Fig. 4.

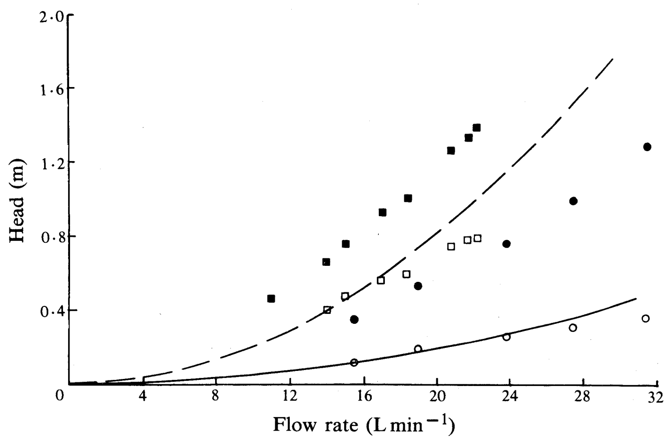

Fig. 6. As for Fig. 5, but with the theoretical curves for $D_3 = 1 \cdot 03$ cm, and with experimental points for $D_3 = 1 \cdot 0$ cm (squares) and for $D_3 = 1 \cdot 2$ cm (circles).

Table 2. Theoretical (t) and experimental (e) flow rates for refilling and pressure-advantage factors β as a function of D_3, with $D_1 = 17$ mm

D_3 (mm)	Starting flow rate (L min^{-1})	β
6·4 (t)	8·1	2·11
6 (e)	7·9	1·6
7·9 (t)	12·5	2·74
8 (e)	12·6	2·0
10 (e)	18·3	1·8
10·3 (t)	22·4	4·18
12 (e)	27·6	3·1
12 (e)	22·5	3·6
10 (e)	17·2	2·0

All theoretical and experimental curves of head loss against flow rate are roughly parabolic, so that the pressure-advantage ratio β is effectively independent of flow rate. In Table 2 we show how β varies with D_3: both theoretically and experimentally, as D_3 increases (i.e. as the constriction becomes more gradual), β increases. We note the low value of β for the 10 mm experimental manifold, which is probably associated with imperfections in the construction (e.g. increased wall roughness introduced during the crimping process). Of course, the starting flow rate associated with h_s reaching $1 \cdot 03$ m increases with D_3. The trade-off between larger starting flow rates and reduced manifold head loss would be decided by practical considerations (such as the characteristics of available pumps).

Experimental Studies of Alternative Single-header Manifolds

Having seen that the manifold of Fig. 3*b* can provide satisfactory flow characteristics, let us see whether these can also be provided by other designs more easily constructed. The simplest possible design (Fig. 3*a*) has already been dismissed, in that it provides riser heads at practicable flow rates which are too small to permit self-draining action. The design of Fig. 3*c* shares the advantage of a uniform header pipe diameter with the design of Fig. 3*a*. It was constructed and tested to determine whether the difference in riser penetration distance x gave an enhanced riser head. As Table 3 shows, the riser head increases with x but remains well below the values for the manifold of Fig. 3*b*. Note that the riser head and riser volume flow rate for the manifold of Fig. 3*c* are roughly independent of the direction of the header flow stream.

Table 3. Static riser heads for various manifolds (D_1 = 17 mm) for two flow rates

Manifold type		Head (m) $Q_h = 16{\cdot}6$ L min^{-1}	$Q_h = 8{\cdot}8$ L min^{-1}
Fig. 3*b*	$D_3 = 12$ mm	0·40	0·13
	= 10	0·90	0·26
	= 8	Flowing	0·55
	= 6	Flowing	Flowing
Fig. 3*c*	$x = 10$ mm	0·17	0·04
	= 15	0·27	0·06
Fig. 3*d*		0·29	0·04
Fig. 3*e*	$D_3 = 12$ mm	0·67	0·33
	= 10	1·00	0·46

The design of Fig. 3*d* generates similar values of riser head to those of Fig. 3*c*, but would be more difficult to construct. For both types of manifold, the pressure-advantage factors are close to unity.

Hybrid designs such as that of Fig. 3*e* combine header constrictions with modifications of the riser geometry. In this way, riser heads and β values may both be increased. The largest β value we have measured of 3·6 was for a manifold of the type Fig. 3*e* (see Table 2).

4. Conclusions

We have considered two different types of self-draining manifold for solar collectors. We have presented simple theoretical models for both types of manifold and shown them to be in general agreement with experimental results. As Table 1 shows, the parallel geometry of the double-header manifold permits smaller refilling heads and operating power losses than the series geometry of the single-header manifold. The latter design offers the compensating advantages of lower materials costs and *a priori* flow balancing in the sense discussed above. Both designs are practical alternatives as self-draining manifolds, with the choice between them depending on factors specific to the site.

Acknowledgments

The authors acknowledge valuable discussions with representatives of Sunmaster Inc. and Solartech Inc. Financial support provided by His Royal Highness Prince Nawaf Bin Abdul Aziz of the Kingdom of Saudi Arabia through the Science Foundation for Physics is gratefully acknowledged.

References

Dubin, F., and Bloome, S. (1981). *In* 'Solar Energy Handbook' (Eds J. F. Kreider and F. Kreith), pp. 13–17 (McGraw–Hill: New York).

Hansen, A. G. (1967). 'Fluid Mechanics', p. 429 (Wiley: New York).

Kreith, F., and Kreider, J. F. (1981). *In* 'Solar Energy Handbook' (Eds J. F. Kreider and F. Kreith), pp. 7–23 (McGraw–Hill: New York).

McPhedran, R. C. (1983). Department of Applied Physics Research Rep. Nos SP 83/1, 83/8 (Univ. of Sydney).

McPhedran, R. C., Mackey, D. J. M., McKenzie, D. R., and Collins, R. E. (1983). *Aust. J. Phys.* **36**, 197–219.

Miller, D. S. (1978). 'Internal Flow Systems', p. 40 (BHRA: London).

Swanson, W. M. (1970). 'Fluid Mechanics', p. 429 (Holt, Rinehart and Winston: New York).

Ward-Smith, A. J. (1980). 'Internal Fluid Flow', p. 307 (Clarendon: Oxford).

Appendix 1. Flow Properties of the Double-header Manifold

We consider fluid entering the manifold of Fig. 1 in the header of internal diameter D_1. We are given the initial header flow rate Q_h^1, so the flow speed v_h^1 before the junction with riser 1 can be found from

$$v_h^1 = 4Q_h^1/\pi D_1^2 . \tag{A1}$$

If we assume a value for the temperature rise ΔT_1 of fluid in its passage between points (i) and (ii) of Fig. 1, we can find the flow speed v_r^1 in riser 1 from

$$v_r^1 = 4P_T/\pi\rho C_V D_r^2 \Delta T_1 , \tag{A2}$$

where P_T is the flow of thermal energy per unit time in the fluid between points (i) and (ii), ρ is its density and C_V its specific heat. The header flow speed V_h^1 after the junction with riser 1 is then

$$V_h^1 = v_h^1 - v_r^1 D_r^2/D_1^2 . \tag{A3}$$

Next, we calculate the fluid pressure P_1 and the dynamic pressure head $\mathscr{P}_1$ at the point (i). To do this, we assume that the pressure P_2 at the point (ii) is equal to the atmospheric pressure P_0, and relate P_1 and P_2 as given by McPhedran *et al.* (1983):

$$P_1/\rho = P_2/\rho + \tfrac{1}{2}(v_r^1)^2(1 + C_{TD} + f_r L_r/D_r) + gL_r \cos\theta , \tag{A4}$$

where we assume laminar riser flow to calculate f_r and take the flow-independent estimate of 0·40 for C_{TD}. The dynamic pressure head $\mathscr{P}_1$ is

$$\mathscr{P}_1 = (P_1 - P_0)/\rho g - L_r \cos\theta \tag{A5}$$

or

$$\mathscr{P}_1 = (v_r^1)^2 \frac{1+C_{TD}}{2g} + \frac{32\mu L_r}{\rho g D_r^2} v_r^1 , \tag{A6}$$

with μ denoting the fluid viscosity.

Having calculated $\mathscr{P}_1$, v_h^1, v_r^1 and V_h^1 for riser 1, we proceed with the corresponding quantities for riser 2. The pressure difference $\mathscr{P}_2 - \mathscr{P}_1$ receives a contribution from frictional losses associated with the header flow (which is assumed completely turbulent), and a second contribution which is a regain term associated with the decrease in header flow speed from v_h^1 to V_h^1:

$$\mathscr{P}_2 = \mathscr{P}_1 - \frac{f L_h (V_h^1)^2}{2 g D_1} + \tfrac{1}{2}\{(v_h^1)^2 - (V_h^1)^2\}, \tag{A7}$$

where f is the header friction factor, for which we use the estimate 0·055. Let us define the two constants for the manifold

$$\alpha = (1 + C_{TD})/2g, \tag{A8}$$

$$\beta = 32 \mu L_r / \rho g D_r^2. \tag{A9}$$

Using the analogue of (A6) for riser 2, we find that

$$v_r^2 = \{-\beta + (\beta^2 + 4\alpha \mathscr{P}_2)^{\frac{1}{2}}\}/2\alpha. \tag{A10}$$

We continue this process by calculating $\mathscr{P}_3$, v_h^3, v_r^3 and V_h^3, stepping along the header until we:

(a) reach the end of the header with a flow speed which differs significantly from zero—this indicates our estimate for ΔT_1 is too large;

(b) fail to reach the end of the header before our flow speed becomes negative—this indicates we should increase ΔT_1; or

(c) we reach the end of the header with a flow speed essentially equal to zero—this indicates the iteration may be terminated, with the calculation of flow properties being complete.

Appendix 2. Flow Properties of a Single-header Manifold

The flow properties of the manifold shown in Fig. 4 are obtained by equating two expressions for the pressure difference $P_3 - P_6$ between $x = L_3$ and L_6. The first of these is obtained by going along the header and, written in terms of known $\bar{v}_2$ and unknown $\bar{v}_3$ flow speeds, this is

$$\Delta P_h = \tfrac{1}{2}\rho (T_1 \bar{v}_2^2 + 2 T_2 \bar{v}_2 \bar{v}_3 + T_3 \bar{v}_3^2), \tag{A11}$$

where, as a consequence of arguments given by McPhedran (1983), the coefficients T_1, T_2 and T_3 are

$$T_1 = 2\gamma_1 - 1 + (1 - 2\gamma_2)(D_2/D_3)^4, \tag{A12}$$

$$T_2 = \gamma_2 (D_2/D_3)^4 - \gamma_1, \tag{A13}$$

$$T_3 = f_3 \frac{L_4 - L_3}{D_3} + \left(\frac{D_2}{D_3}\right)^4 \left(f_4 \frac{L_6 - L_5}{D_3} + K_{SC}\, K_C\right). \tag{A14}$$

Expressions for the flow coefficients γ_1 and γ_2, friction coefficients f_3 and f_4 and the pressure correction coefficient $K_{SC}\, K_C$ have been given by McPhedran (1983).

The expression for $P_3 - P_6$ based on riser flow is

$$\Delta P_r = \tfrac{1}{2}\rho H_r \overline{v}_r^2, \tag{A15}$$

where

$$H_r = 1 + C_{TD} + C_{TC} + K_r + f_r L_r / D_r = M + f_r L_r / D_r, \tag{A16}$$

and where the quantity M is not strongly dependent on the flow speed $\overline{v}_r$. The equation for continuity of flow is

$$\overline{v}_r = (\overline{v}_2 - \overline{v}_3) D_2^2 / D_r^2. \tag{A17}$$

Equating (A11) and (A15) and using (A17), we obtain an equation linking $\overline{v}_3$ and $\overline{v}_2$, which can be solved by a bisection method. Given $\overline{v}_3$, it is a straightforward matter to evaluate ΔP_r and ΔP_t (McPhedran 1983).

Manuscript received 18 February, accepted 18 April 1985